

# Observation of birefringence induced by intersubband transitions in quantum wells

Gilad Almogy, Ali Shakouri, and Amnon Yariv  
California Institute of Technology, Pasadena, California 91125

(Received 25 June 1993; accepted for publication 15 September 1993)

We present a direct measurement of the birefringence induced by the intersubband transitions in quantum wells. Phase delays of up to  $40^\circ$  were observed in our samples, corresponding to a 0.07 difference in the index of refraction between the polarizations parallel and perpendicular to the plane of the wells in a GaAs/AlGaAs silicon-doped structure. The measurement was conducted at several wavelengths—enabling us to deduce the total linear birefringence near the absorption resonance. The observed birefringence is in close agreement with the Kramers–Kronig transform of the absorption spectra.

The first observation of the intersubband transitions (ISBTs) in quantum wells<sup>1</sup> was soon followed with predictions of large, ISBT-induced, birefringence.<sup>2,3</sup> The absorption spectrum of the ISBT has been extensively studied,<sup>4</sup> and applications as infrared detectors,<sup>5</sup> and absorption modulators<sup>6</sup> have been demonstrated. This absorption obeys a simple selection rule, and is observed only for radiation polarized perpendicular to the plane of the quantum wells.<sup>7</sup> The transitions leading to the absorption must also affect the phase velocities, i.e., the index of refraction, where the two effects are connected by the Kramers–Kronig relations.<sup>8</sup> Thus the large, controllable, and polarization-sensitive absorption of ISBTs leads to an expectation of a large birefringence at selected wavelengths. In this letter, we report on the experimental observation of this ISBT-induced birefringence in a GaAs/AlGaAs silicon-doped quantum-well structure.

Because of these polarization-dependent transitions, and the accompanying changes of the index of refraction, the quantum-well stack acts as a uniaxial crystal. To measure the birefringence, that is, the index of refraction difference between polarizations interacting with the ISBT (perpendicular to the plane of the quantum wells) and not interacting with the ISBT (in the plane of the quantum wells), a beam is propagated at a  $45^\circ$  angle relative to the plane of the quantum wells (Fig. 1). This configuration offers a large interaction with the ISBT, but leads to a structural phase shift which is due to the different reflection phases of the *s* and *p* polarization components in the total internal reflections of the GaAs-air interface. To account for this effect, the total phase delay was measured at several wavelengths, and the strongly wavelength-dependent ISBT contribution was isolated from the nearly wavelength-independent structural contribution. Despite the structural phase factor, propagation at  $45^\circ$  still lends itself more readily to birefringence measurements than the other standard schemes for interaction with the ISBT (waveguide, Brewster angle), as it leads to a large interaction and the structural phase factor is essentially wavelength dependent.<sup>9</sup>

To calculate the expected linear birefringence we apply the standard two-level model<sup>8</sup> for the linear polarization induced by an electromagnetic field of frequency  $\omega$ , inter-

acting with the ISBT. This leads to an imaginary component ( $\chi''$ ) and a real component ( $\chi'$ ) of the susceptibility (related by the Kramers–Kronig relations), given as

$$\chi''(\omega) = \frac{\mu^2 \Delta N}{2\epsilon_0 \hbar} \frac{1}{T_2} \frac{1}{(\omega - \omega_0)^2 + (1/T_2)^2} \quad (1a)$$

and

$$\chi'(\omega) = \frac{\mu^2 \Delta N}{2\epsilon_0 \hbar} \frac{(\omega - \omega_0)}{(\omega - \omega_0)^2 + (1/T_2)^2}, \quad (1b)$$

where  $\epsilon_0$  is the vacuum permittivity,  $\Delta N$  is the population difference between the subbands,  $\omega_0$  is the transition frequency,  $T_2$  is the dephasing time, and  $\mu$  is the intersubband dipole matrix element. For polarizations at an angle normal to the quantum-well planes the effective dipole matrix elements are scaled down by the cosine of that angle due to the selection rule. From the susceptibility, the absorption coefficient (for amplitudes) of the ISBT is given by

$$\alpha(\omega) = \frac{1}{2} \frac{\omega}{nc} \chi''(\omega) \quad (2a)$$

and the change in the index of refraction is

$$\Delta n(\omega) = n \sqrt{1 + \frac{\chi'(\omega)}{n^2}} - n \cong \frac{\chi'(\omega)}{2n}, \quad (2b)$$

where  $n$  is the bulk index of refraction.

In the configuration shown in Fig. 1, an input field of amplitude  $E_{in}$ , propagating at a  $45^\circ$  angle relative to the plane of the wells and polarized at an angle of  $\phi$  with respect to the normal to the plane of propagation, the output amplitude is

$$E_{out}(t) = E_{in} \exp \left[ i \left( \omega t - \frac{\omega n}{c} L_b \right) - \alpha_b L_b \right] \\ \times \left[ \cos \phi \exp \left( -\alpha(\omega) L_{QW} - \frac{i\omega}{c} \Delta n(\omega) L_{QW} + i\varphi_g \right) \hat{y} + \sin \phi \hat{x} \right],$$

where  $\alpha_b$  and  $L_b$  are the bulk absorption coefficient and bulk propagation length, respectively, and we have taken the polarization-independent bulk contribution outside the

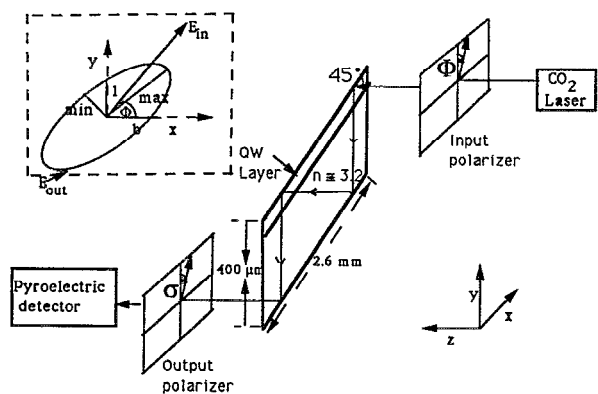


FIG. 1. The propagation of the beam in the 45° bounce scheme. The inset displays the input light, linearly polarized at an angle  $\Phi$ , and the output elliptical polarization.

parenthesis.  $\varphi_g$  is the structural phase delay, and  $L_{QW}$  is the propagation length in the active well region that is proportional to the number of bounces in the sample ( $n_b$ ). Care must be taken to keep this number constant throughout the experiment, preferably uniform across the beam.

The structural phase factor due to the difference in the phase of the total internal reflections of the  $s$  and  $p$  polarizations is

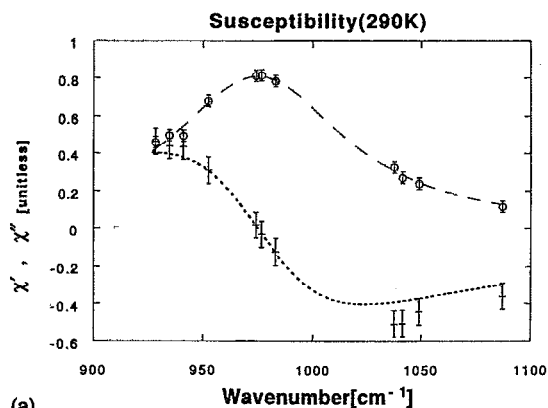
$$\varphi_g = 2n_b \tan^{-1} \left( \frac{\cos \theta_i \sqrt{\sin^2(\theta_i) - 1/n^2}}{\sin^2(\theta_i)} \right), \quad (4)$$

where  $\theta_i$  is the angle of incidence—45° in this case. In the reflection of a  $\lambda \approx 10 \mu\text{m}$  beam from a GaAs-air interface, there will be a relative phase delay of approximately 83° between the two components of the polarization. This phase delay is negligibly wavelength dependent over the wavelength range of our experiment (9.2–10.75  $\mu\text{m}$ ), so the total phase delay  $\varphi_T(\omega)$ , is

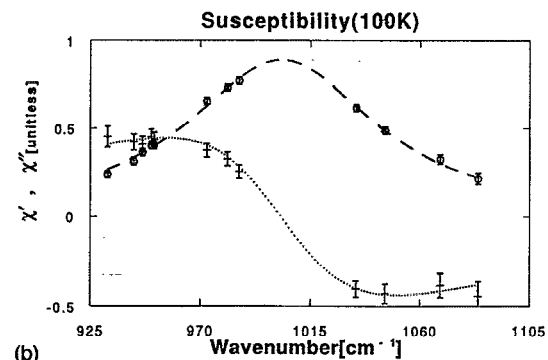
$$\varphi_T(\omega) = \frac{\omega \Delta n(\omega)}{c} L_{QW} + \varphi_g. \quad (5)$$

To maximize the dependence of the index of refraction on the wavelength, the sample was chosen to have its absorption peak around 10  $\mu\text{m}$ —in the middle of the CO<sub>2</sub> laser's spectral range. Thirty periods of GaAs 70 Å quantum wells, silicon doped to  $3 \times 10^{18} \text{ cm}^{-3}$ , with 440 Å GaAl<sub>0.3</sub>As barriers were grown by molecular beam epitaxy on a semi-insulating GaAs substrate. The results presented in Fig. 2 are for a 2.6-mm-long, 400- $\mu\text{m}$ -thick sample, lapped at 45° angles on both facets.

The experiment, shown in Fig. 1, was carried out at room temperature, and with a Joule-Thompson cooler at 100 K. The expected shift and narrowing of the absorption peak,<sup>10</sup> and the real part of the susceptibility along with it, allowed us to include different parts of the birefringence curve within our laser's spectral range on the same sample, enabling separation between the intersubband and structurally induced phase delays. An air cooled, grating tunable, cw CO<sub>2</sub> laser with an output of 3 W is transmitted through a Brewster angle polarizer. The linearly polarized



(a)



(b)

FIG. 2. The measured polarization-dependent real and imaginary components of the susceptibility as a function of wavelength at 290 K (a) and 100 K (b). The dashed line is a Lorentzian fit to the imaginary part of the susceptibility corresponding to the ISBT absorption. The dotted line is a Kramers-Kronig transform of the dashed line—the expected real part of the susceptibility.

beam is focused on the sample with a 254 mm ZnSe lens. In the sample, the beam propagates at a 45° angle with respect to the plane of the wells and undergoes several total internal reflections. The output beam is then passed through a wire grid polarizer and focused on a pyroelectric detector, whose signal was locked to the trigger of a mechanical chopper. A low duty cycle was used to prevent thermal effects, and laser power on the sample never exceeded 1/100 of the saturation intensity—preventing significant nonlinear effects. A 100  $\mu\text{m}$  aperture was placed in front of the sample to eliminate variation in effective number of bounces ( $n_b$ ) due to beam displacements.

The detector power as a function of the cross-polarizer rotation angle  $\sigma$  with respect to the plane of the quantum wells (see Fig. 1) is proportional to

$$P(\sigma) \sim \cos^2 \sigma + b^2 \sin^2 \sigma + 2b \cos \sigma \sin \sigma \cos \varphi_T, \quad (6)$$

where  $b$  is defined as the ratio of the  $x$  and  $y$  components of the field

$$b = \frac{E_x}{E_y} = \tan \phi e^{-[\alpha(\omega)/2] L_{QW}}. \quad (7)$$

The ISBT absorption is measured by comparing the transmittance at the interacting ( $y$ ), and noninteracting ( $x$ ) polarizations. Figure 2 shows the resultant measured imaginary part of the susceptibility with its Lorentzian fit

[Eq. (1a)] at room temperature and at 100 K. The best fits are given by a resonance at  $976\text{ cm}^{-1}$  ( $10.25\text{ }\mu\text{m}$ ), with  $54\text{ cm}^{-1}$  broadening at room temperature, and resonance at  $1002\text{ cm}^{-1}$  ( $9.98\text{ }\mu\text{m}$ ), with  $48\text{ cm}^{-1}$  broadening at 100 K. Consistent with the Kramers–Kronig relations, the parameters of this fit were used to calculate the expected real part of the susceptibility [Eq. (1b)]—shown in Fig. 2. The total phase delay induced by the structure:  $\varphi_T$ , is determined (to a factor of  $2\pi m \pm \varphi_T$ ) by the measured ratio of the maximum to the minimum powers of the elliptically polarized output for a given  $b$  (see the inset of Fig. 1). A constant structural phase term ( $\varphi_g$ ) is now subtracted from these measurements for a best fit with the absorption curve's transformation. A fit was obtained after a subtraction of the structural phase delay, found to be  $2\pi m - 97^\circ$  at room temperature, and  $2\pi m - 93^\circ$  at 100 K. A value of  $n_b \cong 7.5$  (i.e., not uniform throughout the cross section of the beam), is consistent with this phase delay, and with the sample's height/length ratio. Figure 2 shows an excellent agreement between measured real and imaginary components of the susceptibility at 100 K, and a fairly good agreement at room temperature. For verification, the laser absorption measurements are compared to Fourier transform infrared results and found to be in close agreement. The experiment was repeated for a sample with a peak outside the laser's spectral range ( $8.6\text{ }\mu\text{m}$ ), and for bulk GaAs to validate the assumption of a nearly frequency-independent structural phase factor.

The maximal ISBT-induced phase delay, about  $40^\circ$ , is found, as expected, at the absorption's half-maximum points. Following the standard convention for quantum-well absorption, presenting the birefringence per unit length of the quantum-well stack, this translates to a change in the index of refraction of  $\Delta n = 0.07$ . Since our samples were grown with very thick barriers, an artificial improvement by a factor of 3 through narrower barriers is

easily attainable. Interaction at a right angle, rather than at a  $45^\circ$  angle with the plane of the wells—will double the birefringence just as the absorption. Thus a refractive index change as high as 0.4 seems attainable.

The birefringence measurement suggests the feasibility of phase modulation of mid-IR radiation through the large refractive index nonlinearities induced by the ISBTs. Since the ISBTs have been shown to be highly controllable,<sup>6</sup> the birefringence may be shifted by dc fields, or saturated by ac fields, and thus gives the upper limit to realizable ISBT nonlinearities.<sup>11</sup> Near the absorption peak, modulation of phase and absorption are, of course, coupled, but the magnitude of the absorption peak varies as the inverse square of the detuning, whereas that of the birefringence decreases only linearly; thus the birefringence dominates far from resonance. When the index change is maximized it should be sufficient for effective modulation far from resonance. Attempts at such modulation are currently underway.

- <sup>1</sup>L. C. West and S. J. Eglash, *Appl. Phys. Lett.* **46**, 1153 (1985).
- <sup>2</sup>D. Ahn and S. L. Chuang, *IEEE J. Quantum Electron.* **QE-23**, 2196 (1987).
- <sup>3</sup>K. J. Khun, G. U. Iyengar, and S. Yee, *J. Appl. Phys.* **70**, 5010 (1991).
- <sup>4</sup>G. Bastard, E. E. Mendez, L. L. Chang, and L. Esaki, *Phys. Rev. B* **28**, 3241 (1983).
- <sup>5</sup>J. S. Smith, L. C. Chiu, S. Margalit, A. Yariv, and Y. Cho, *J. Vac. Sci. Technol. B* **1**, 376 (1983).
- <sup>6</sup>E. Martinet, L. E. Rosener, P. Bois, and S. Delaitre, *Appl. Phys. Lett.* **60** (7), 895 (1992); and: R. P. G. Karunasiri, Y. J. Mii, and K. L. Wang, *IEEE Electron Device Lett.* **EDL-11**, 227 (1990).
- <sup>7</sup>Within the single band model analysis, applicable when the ISBTs are between confined conduction band states in GaAs/AlGaAs structures: A. Shik, in *Intersubband Transitions in Quantum Wells*, edited by E. Rosener (Plenum, New York, 1992), p. 319.
- <sup>8</sup>A. Yariv, *Quantum Electronics* (Wiley, New York, 1989).
- <sup>9</sup>D. D. Yang, F. H. Julien, P. Boucaud, J. M. Lourtios, and R. Paniel, *IEEE Photon Technol. Lett.* **PTL-2**, 181 (1990).
- <sup>10</sup>M. O. Manasreh, F. Szmulowicz, D. A. Fisher, K. R. Evans, and C. E. Stutz, *Appl. Phys. Lett.* **57**, 1790 (1990).
- <sup>11</sup>G. Almog, M. Segev, and A. Yariv, *Phys. Rev. B* **15**, 10950 (1993).